



Since January 2020 Elsevier has created a COVID-19 resource centre with free information in English and Mandarin on the novel coronavirus COVID-19. The COVID-19 resource centre is hosted on Elsevier Connect, the company's public news and information website.

Elsevier hereby grants permission to make all its COVID-19-related research that is available on the COVID-19 resource centre - including this research content - immediately available in PubMed Central and other publicly funded repositories, such as the WHO COVID database with rights for unrestricted research re-use and analyses in any form or by any means with acknowledgement of the original source. These permissions are granted for free by Elsevier for as long as the COVID-19 resource centre remains active.

# Removal of fine and ultrafine particles from indoor air environments by the unipolar ion emission

Byung Uk Lee, Mikhail Yermakov, Sergey A. Grinshpun\*

*Department of Environmental Health, Center for Health-Related Aerosol Studies, University of Cincinnati, 3223 Eden Avenue, PO Box 670056, Cincinnati, OH 45267-0056, USA*

Received 8 March 2004; accepted 15 June 2004

## Abstract

The continuous emission of unipolar ions was evaluated in order to determine its ability to remove fine and ultrafine particles from indoor air environments. The evolution of the indoor aerosol concentration and particle size distribution was measured in real time with the ELPI in a room-size ( $24.3\text{ m}^3$ ) test chamber where the ion emitter was operating. After the results were compared with the natural decay, the air cleaning factor was determined. The particle aerodynamic size range of  $\sim 0.04\text{--}2\text{ }\mu\text{m}$  was targeted because it represents many bioaerosol agents that cause emerging diseases, as well as those that can be used for biological warfare or in the event of bioterrorism. The particle electric charge distribution (also measured in the test chamber with the ELPI) was rapidly affected by the ion emission. It was concluded that the corona discharge ion emitters (either positive or negative), which are capable of creating an ion density of  $10^5\text{--}10^6\text{ e}^\pm\text{ cm}^{-3}$ , can be efficient in controlling fine and ultrafine aerosol pollutants in indoor air environments, such as a typical office or residential room. At a high ion emission rate, the particle mobility becomes sufficient so that the particle migration results in their deposition on the walls and other indoor surfaces. Within the tested ranges of the particle size and ion density, the particles were charged primarily due to the diffusion charging mechanism. The particle removal efficiency was not significantly affected by the particle size, while it increased with increasing ion emission rate and the time of emission. The performance characteristics of three commercially available ionic air purifiers, which produce unipolar ions by corona discharge at relatively high emission rates, were evaluated. A 30-minute operation of the most powerful device among those tested resulted in the removal of about 97% of  $0.1\text{ }\mu\text{m}$  particles and about 95% of  $1\text{ }\mu\text{m}$  particles from the air in addition to the natural decay effect.

© 2004 Elsevier Ltd. All rights reserved.

*Keywords:* Indoor environment; Air purification; Aerosol concentration; Unipolar ion emission; Electric charge

## 1. Introduction

Numerous epidemiological studies have established an association between the indoor aerosol contaminants,

including airborne dust, bioaerosols and aeroallergens, and adverse health effects. Most of respiratory problems are closely associated with fine ( $\leq 2\text{ }\mu\text{m}$ , Baron and Willeke, 2001) and ultrafine ( $\leq 0.1\text{ }\mu\text{m}$ , Hinds, 1999) particle size fractions. Given that people spend a significant percentage of their time indoors (Klepeis et al., 2001), there is a high demand for efficient methods for indoor air cleaning against fine and ultrafine aerosol particles. Conventional techniques for controlling

\*Corresponding author. Tel.: 1-513-558-0504; fax: 1-513-558-2263.

*E-mail address:* [sergey.grinshpun@uc.edu](mailto:sergey.grinshpun@uc.edu)  
(S.A. Grinshpun).

indoor aerosol pollutants, including mechanical filtration and electrostatic precipitation, have been incorporated into commercial devices of various capacities and efficacies (Ludwig and Turner, 1991). While being widely and successfully used in indoor air environments, the mechanical devices and electrostatic precipitators are often criticized for their considerable size and power consumption, excessive noise level, and the need to be routinely maintained (e.g., routine filter replacement and the plate cleaning). Electrostatic filters have also been used for air cleaning but there have been very few studies that characterized their efficiency with a particular focus on fine and ultrafine particles (Jamriska et al., 1998).

As an alternative method, the emission of air ions that charges aerosol particles has been evaluated as to its capability to reduce the concentration of airborne dust and microorganisms in indoor environments (Grabarczyk, 2001; Grinshpun et al., 2001; Krueger and Reed, 1976; Niu et al., 2001). Among several particle charging methods, corona ionization is particularly effective in charging small aerosol particles, including the fine and ultrafine fractions (Adachi et al., 1985; Buscher et al., 1994; Wiedensohler et al., 1994; Hernandez-Sierra et al., 2003). Recent experiments conducted in a 2.6 m<sup>3</sup> test chamber with a manikin have demonstrated that the aerosol concentration in the breathing zone may decrease considerably due to unipolar ion emission with a corona ionizer (Grinshpun et al., 2004). In these experiments, the concentration and the size distribution of 0.3–3 μm particles aerosolized by a Collison nebulizer (BGI, Inc., Waltham, MA, USA) were measured in real time using an optical particle counter. It was concluded that the aerosol particles, charged unipolarly by the emitted ions, repel and migrate toward the indoor surfaces, which results in their rapid deposition on these surfaces. Thus, it is anticipated that the efficiency of air cleaning in an indoor air environments depends on its volume.

Those ion emitters, which meet health standards (e.g., do not generate ozone above the established thresholds), have been incorporated in commercial air purification devices. The air purifiers that apply either open or shielded corona ionizers are being increasingly used in indoor environments. Nevertheless, there is a lot of controversial information about the performance of these devices, and the claims made by some manufacturers have not been substantiated by credible scientific investigations. Available ionic air purifiers differ by the emission rate, ion polarity (either unipolar or bipolar), and other characteristics.

The data reported earlier by our research group (Grinshpun et al., 2001, 2004) revealed that a high-density unipolar ion emission has a good potential for air cleaning in confined spaces, such as a very small room or a car cabin (volume ~1–10 m<sup>3</sup>). However, the efficiency of this method for larger volumes (e.g., a

typical room of 20–40 m<sup>3</sup>) has not been quantitatively characterized. Furthermore, no information has been reported on the efficiency of the unipolar ionic air purification against the particles of ≤0.3 μm, which includes the ultrafine fraction and the lower end of the fine fraction.

In this study, we investigated the effect of continuous unipolar ionization on the evolution of the indoor concentration and particle size distribution of fine and ultrafine aerosols. We targeted the particle aerodynamic diameter range of  $d_a \sim 0.04\text{--}2\ \mu\text{m}$ , which is of special public interest because of its health relevance. Many bioaerosol agents that cause emerging diseases, as well as those that can be used for biological warfare or in the event of bioterrorism, belong to this particle size range. For example,  $d_a \sim 0.1\ \mu\text{m}$  for *coronavirus* (the etiological agent of the SARS) and  $d_a \sim 1\ \mu\text{m}$  for *Bacillus anthracis* (bacteria causing anthrax). Three ion emitters, VI-2500, AS150MM (+), and AS150MM (–), which produce unipolar ions by corona discharge at different emission rate and polarity (all are available from Wein Products Inc., Los Angeles, CA, USA), were evaluated in a room-size indoor chamber. The aerosol concentration and aerodynamic particle size distribution in the chamber were monitored in real time. The particle electric charge distribution was also measured to relate the ion emission rate to the particle removal efficiency.

## 2. Method

The tests were conducted in a non-occupied, unventilated test chamber ( $L \times W \times H = 3.78\ \text{m} \times 2.44\ \text{m} \times 2.64\ \text{m} = 24.3\ \text{m}^3$ ). This facility was developed in the Center for Health-Related Aerosol Studies at the University of Cincinnati and used in our previous studies (Choe et al., 2000; Grinshpun et al., 2002). A closed-loop air ventilation system with two HEPA filtration units was utilized to clean the chamber between experiments. A small fan was used to achieve a uniform aerosol concentration pattern inside the chamber.

The electrical low pressure impactor (ELPI, TSI Inc./Dekati Ltd, St. Paul, MN, USA) was used to determine the concentration and aerodynamic particle size distribution in real-time. This instrument utilizes the cascade impaction principle and also has a direct-reading capability. When performing the concentration and size distribution measurements, the particles were directed to the ELPI inlet through the Kr<sup>85</sup> charge equilibrator (3M Company, St. Paul, MN, USA). The ELPI is also capable of measuring the charge distribution of the collected particles. When the instrument was used in the charge-detection mode, the Kr<sup>85</sup> charge equilibrator was detached from the system. The time resolution of the ELPI was adjusted to 10 s. The data were recorded in 12 ELPI channels (each channel

= impaction stage), from 0.04 to 8.4  $\mu\text{m}$ . The latter sizes represent the midpoint diameters of the respective impaction stages (the midpoint = the geometric mean of the stage's boundaries). The ELPI operated in the center of the chamber.

The natural aerosol concentration in the chamber was not sufficiently high for accurate direct-reading measurements, especially after the first 5–10 min of the operation of an ion emitter, which removed a considerable number of airborne particles. To increase the initial background aerosol concentration, we used a smoke generator. The generated smoke particles primarily covered a submicrometer aerodynamic size range (Cheng et al., 1995). Overall, the data recorded in the first 9 measurement channels of the ELPI ( $d_a = 0.04\text{--}2.0 \mu\text{m}$ ) were sufficient.

Three ion emitters were tested: a stationary negative ionic air purifier, VI-2500 ( $L \times W \times H = 20 \text{ cm} \times 16.5 \text{ cm} \times 8.5 \text{ cm}$ ), as well as two portable purifiers, positive AS150MM (+) and negative AS150MM (–) ( $L \times W \times H = 6.5 \text{ cm} \times 4 \text{ cm} \times 2.2 \text{ cm}$ ). The ion density produced by the non-thermal corona discharge in the chamber was measured in our experiments for each device with the Air Ion Counter (AlphaLab Inc., Salt Lake City, UT, USA) continuously every 10 s during about an hour. This device is capable of measuring within the range of  $10^1\text{--}2 \times 10^6 \text{ ions cm}^{-3}$ .

First, the natural decay of the aerosol concentration was determined. Prior to the test, the smoke aerosol was generated and mixed in the chamber for 20 min so that it was uniformly distributed and the average total particle concentration exceeded the level of  $\sim 1.3 \times 10^5 \text{ cm}^{-3}$ . Then the ELPI began recording the data ( $t = 0$ ) starting from the initial concentration  $C_{\text{initial}}(d_a, t = 0)$ . It operated continuously for 1 h, and the aerosol concentration  $C_{\text{natural}}(d_a, t)$  was measured. To quantitatively characterize the natural decay, the non-dimensional fractional concentrations

$$\overline{c_{\text{natural}}} = \frac{C_{\text{natural}}(d_a, t)}{C_{\text{initial}}(d_a, t = 0)} \quad (1)$$

were determined every 10 s.

After this, the test aerosol was generated and mixed in the chamber again to reach the same initial concentration level. At  $t = 0$ , the ion emitter located in the center of the chamber was turned on and  $C_{\text{initial, ionizer}}(d_a, t = 0)$  was determined (the distance from the ion emitter to the inlet of the ELPI was approximately 0.2 m). Then the aerosol concentration,  $C_{\text{ionizer}}(d_a, t)$ , was measured with the ELPI in a 10-second time intervals during 1 h, until the particle count decreased below the limit of detection.

The chamber was cleaned by a close-loop ventilation system at 10 air exchanges per hour for about 4 h to insure that the ions generated during the test had been

removed and the initial natural aerosol concentration in the chamber had been restored. Then the experimental procedure was repeated for the next ion emitter under the test program.

The air temperature was  $23 \pm 1^\circ\text{C}$  and the relative humidity was  $42 \pm 9\%$  during each experiment as monitored with a Thermometer/hygrometer (Tandy Co., Fort Worth, TX, USA).

To quantify the efficiency of the particle removal exclusively due to the ion emission, the air cleaning factor (ACF) was determined. For every particle size, ACF is defined as the ratio of the concentration measured at a specific time point during the natural decay to the concentration measured at the same time point when the ion emitter was operating:

$$\text{ACF} = \frac{C_{\text{natural}}(d_a, t)}{C_{\text{ionizer}}(d_a, t)}. \quad (2)$$

The data on ACF were presented as a function of the particle aerodynamic size and the duration of the ion emission. The aerosol concentrations  $C_{\text{ionizer}}(d_a, t)$  were also compared to  $C_{\text{initial, ionizer}}(d_a, t = 0)$ , and the decay was characterized by the non-dimensional concentration

$$\overline{c_{\text{ionizer}}} = \frac{C_{\text{ionizer}}(d_a, t)}{C_{\text{initial, ionizer}}(d_a, t = 0)}. \quad (3)$$

In addition to the particle size and concentration measurements, the particle charges were measured with the ELPI that operated in its electrical charge detection mode. The data were revealed using the software made available by Dekati, Ltd., Tampere, Finland. The particle charge distribution was also assessed using the diffusion charging model (Hinds, 1999):

$$n(t) = \frac{d_p k T}{2 K_E e^2} \ln \left[ 1 + \frac{\pi K_E d_p c_i e^2 N_i t}{2 k T} \right] \quad (4)$$

where  $n(t)$  is the number of elementary charges acquired by a particle during a time  $t$  due to the diffusion charging;  $d_p$  is the particle physical diameter;  $k = 1.38 \times 10^{-23} \text{ J K}^{-1}$  is the Boltzmann's constant;  $T$  is the air temperature (K);  $K_E = 9.0 \times 10^9 \text{ N m}^2 \text{ C}^{-2}$  is a constant of proportionality of the *Coulomb's* electrostatic equation;  $e = 1.6 \times 10^{-19} \text{ C}$  is the elementary charge;  $c_i$  is the mean thermal speed of ions; and  $N_i$  is the ion density in the air. In our calculations, we assumed that  $d_p \approx d_a$  since the particles were close-to-spherical and their density was  $1 \text{ g cm}^{-3}$  (Cheng et al., 1995).

The average values and the standard deviations were calculated for each set of conditions as a result of at least 3 replicates. The data were statistically analyzed using the Microsoft Excel software package (Microsoft Co., Redmond, WA, USA).

### 3. Results and discussion

Fig. 1 shows the initial particle size distribution. The data represent the average of 9 tests. It is seen that the particles of  $d_a \approx 0.04\text{--}0.5\ \mu\text{m}$  were dominant ( $\Delta C/\Delta \log d_a$  ranged from  $\sim 10^4$  to  $> 10^5\ \text{cm}^{-3}$ ), while larger particles of  $d_a \approx 1\text{--}2\ \mu\text{m}$  were present at lower concentration levels ( $\Delta C/\Delta \log d_a \sim 10^2\text{--}10^3\ \text{cm}^{-3}$ ). The initial ( $t=0$ ) aerosol concentration of each measured particle size fraction was reproducible with the variability not exceeding 40% for 9 replicates.

The evolution of the non-dimensional particle fractional concentration due to the natural decay is shown in Fig. 2. The non-monotonic fractional decay curves reflect the variety of physical mechanisms involved in the aerosol transport even if no ventilation is introduced in the indoor environment (Vincent, 1995). The particles of smaller ( $d_a < 0.2\ \mu\text{m}$ ) and larger ( $d_a > 0.8\ \mu\text{m}$ ) fractions demonstrated greater decay than those of an intermediate range. The smaller particles are naturally removed from the air through depositing on indoor surfaces primarily due to the effect of diffusion, which becomes more pronounced with the decreasing particle size. In addition, the aerosol concentration of smaller particles decreases due to their coagulation with larger ones. The larger particles are subjected to the inertial deposition and gravitational sedimentation, which both increase with the increasing particle size. The above effects are relatively weak in the intermediate size range of  $\approx 0.2\text{--}0.8\ \mu\text{m}$ . The available gravitational settling models [tranquil or stirred (Hinds, 1999)] cannot accurately predict the natural decay rate observed in this study (in the absence of air ionization by an emitter). Our experimental data demonstrated that the concentration decay was twice as rapid as had been predicted by the above models for larger particles. This difference may be attributed to the intrinsic flow instability associated with

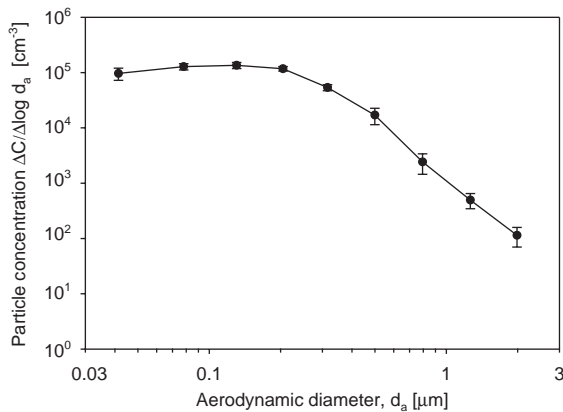


Fig. 1. The initial particle size distribution. The error bars represent the standard deviations of 9 replicates.

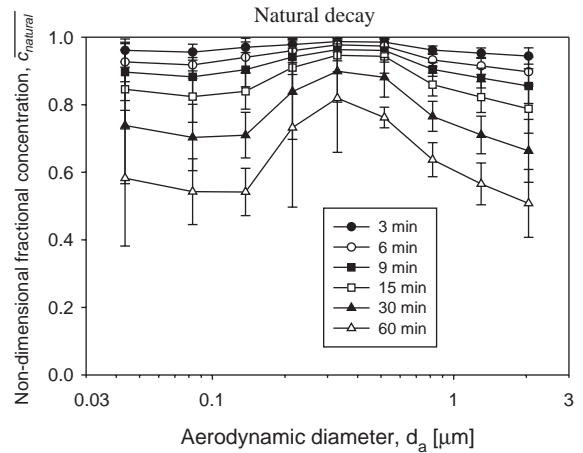


Fig. 2. The evolution of the non-dimensional particle fractional concentration during natural decay. The error bars represent the standard deviations of 3 replicates.

the ELPI operation and other factors that enhance the particle deposition on surfaces. Also, the experimental equipment inside the chamber introduced some extra indoor surfaces, in addition to the floor, thereby increasing the natural particle deposition rate as compared to the gravitational settling models.

Although the natural decay shown in Fig. 2 for the fine and ultrafine particles is sharper than it is predicted by theoretical models, it is still very slow for effective air cleaning: it takes 30 min to achieve a concentration decrease by about 10–30% and an hour to achieve approximately 20–50% drop.

The unipolar ion emission may accelerate the aerosol concentration decay significantly. The air cleaning factors are presented in Table 1a for VI-2500 and Table 1b for AS150MM (+) and AS150MM (–). Resulting from a 15-minute operation of the VI-2500 (which has the highest emission rate among the tested ionic air purifiers), the particles were removed from indoor air at the rate, which is greater than the natural decay rate by a factor of  $5.0 \pm 1.1$  to  $6.8 \pm 0.7$ . A 30-minute operation of VI-2500 surpassed the natural decay rate by a factor ranging from  $15.3 \pm 2.6$  to  $33.6 \pm 5.5$ . This resulted in the removal of about 97% of  $0.1\ \mu\text{m}$  particles and about 95% of  $1\ \mu\text{m}$  particles from the air, in addition to the natural aerosol concentration decrease that occurred during the same time. The positive ion emission produced by AS150MM (+) and the negative ion emission produced by AS150MM (–) also significantly cleaned indoor air from the particles of  $0.04\text{--}2\ \mu\text{m}$ , but the ACF-values were not as high as those obtained for the more powerful VI-2500 (see Table 1). The difference between the data obtained for AS150MM(+) and AS150MM(–) was statistically insignificant. The arithmetic average of the

Table 1

The air cleaning factor (ACF) provided by continuous operation of the ion emitter: (a) VI-2500 and (b) AS150 mm (+)/(-)

Aerodynamic particle diameter ( $\mu\text{m}$ )	Air cleaning factor					
	15 min		30 min		60 min	
(a) VI-2500						
0.04			5.2 $\pm$ 2.6		15.3 $\pm$ 2.6	
0.1			6.8 $\pm$ 0.7		31.0 $\pm$ 2.0	
0.2			6.7 $\pm$ 0.5		33.6 $\pm$ 5.5	
0.5			5.7 $\pm$ 1.1		25.8 $\pm$ 7.3	
1			5.0 $\pm$ 1.1		18.7 $\pm$ 3.6	
2			5.3 $\pm$ 1.7		22.1 $\pm$ 5.1	
Aerodynamic particle diameter ( $\mu\text{m}$ )	Air cleaning factor					
	15 min		30 min		60 min	
	AS150MM (+)	AS150MM (-)	AS150MM (+)	AS150MM (-)	AS150MM (+)	AS150MM (-)
(b) AS150MM(+)/(-)						
0.04	1.4 $\pm$ 0.3	1.2 $\pm$ 0.2	2.1 $\pm$ 0.4	1.8 $\pm$ 0.2	3.9 $\pm$ 0.8	3.9 $\pm$ 0.2
0.1	1.9 $\pm$ 0.3	1.7 $\pm$ 0.2	2.9 $\pm$ 0.6	2.7 $\pm$ 0.3	5.9 $\pm$ 1.3	6.4 $\pm$ 0.5
0.2	1.5 $\pm$ 0.1	1.4 $\pm$ 0.1	2.3 $\pm$ 0.4	2.3 $\pm$ 0.2	5.4 $\pm$ 1.4	6.2 $\pm$ 0.4
0.5	1.9 $\pm$ 0.9	2.3 $\pm$ 1.1	2.9 $\pm$ 1.4	3.4 $\pm$ 1.6	5.5 $\pm$ 2.2	7.2 $\pm$ 2.8
1	1.9 $\pm$ 0.6	2.2 $\pm$ 1.0	2.6 $\pm$ 0.8	3.1 $\pm$ 1.2	4.7 $\pm$ 1.0	5.9 $\pm$ 1.9
2	2.3 $\pm$ 0.7	2.4 $\pm$ 0.9	3.0 $\pm$ 1.0	3.2 $\pm$ 1.1	4.7 $\pm$ 1.1	5.6 $\pm$ 1.6

$p$ -values that represented each particle size fraction was  $\bar{p} = 0.19$ . In a 30-minute operation of AS150MM, the air cleaning rate surpassed the natural decay by a factor ranging from  $2.1 \pm 0.4$  to  $3.4 \pm 1.6$ . A 60-minute operation of both AS150MM devices allowed reaching about twice greater ACF-values than their 30-minute operation. No statistically significant effect of the particle aerodynamic size on the air cleaning factor was observed ( $\bar{p} = 0.18$ ).

The evolution of the non-dimensional particle fractional concentration with the time of ion emission is shown in Fig. 3 as a function of  $d_a$ : VI-2500 (Fig. 3a), AS150MM (+) (Fig. 3b), and AS150MM (-) (Fig. 3c). To standardize the ion emission rate characteristics of different emitters, we measured  $N_i$  with the Air Ion Counter at a distance of 1 m from the source during the test. The ion densities provided by VI-2500, AS150MM (+), and AS150MM (-) were  $(1.34 \pm 0.04) \times 10^6 \text{ e}^- \text{ cm}^{-3}$ ,  $(3.62 \pm 0.18) \times 10^5 \text{ e}^+ \text{ cm}^{-3}$ , and  $(3.91 \pm 0.22) \times 10^5 \text{ e}^- \text{ cm}^{-3}$ , respectively. The numbers in parenthesis in Fig. 3 indicate an average value of the measured  $N_i$  (in elementary charges per  $\text{cm}^3$ ). For each device, the ion emission during the first 3 min resulted in a statistically significant decrease of the aerosol concentration across the tested particle size range ( $\bar{p} = 0.03$ ). Continuous ion emission [an “ion shower” as referred to by Grabarczyk (2001)] makes the particle removal effect time-dependent. Resulting from the continuous operation of VI-2500, the aerosol concentra-

tion decreased more than 2-fold in 6 min, ~3-fold in 9 min, ~5 to 10-fold in 15 min, and >20-fold in 30 min. Both the positive and negative AS150MM ion emitters also efficiently removed particles from indoor air, but not as rapidly as the more powerful VI-2500. The above decrease of the particle concentration was observed for the entire test particle size range. No significant effect of the particle size on the efficiency of air cleaning was found ( $\bar{p} = 0.17$ ).

It was found that the particle electric charges of the initially generated aerosol were very low. On average, the ELPI measured less than one elementary charge per particle. In contrast, when an ion emitter operated, the airborne particles exhibited considerable charges (either positive or negative, depending on the polarity of the emitter). The particle charge distributions measured experimentally by the ELPI and calculated using Eq. (4) are presented in Fig. 4 in a logarithmic scale. The graphs represent the data obtained after the ionizers were operated for 3 min. It is seen that the average particle charge increases sharply with its size. The ion emission from VI-2500 increased the initial particle electric charges to ~ $10^1$  negative elementary charges per particle of 0.1  $\mu\text{m}$  and to ~ $10^2$  negative elementary charges per particle of 1  $\mu\text{m}$ . The ions emission from the AS150MM devices resulted in a lower, but still significant particle charge enhancement. The average deviations between the experimental results and the theoretical data across the entire test particle size range were about 31%, 23%,

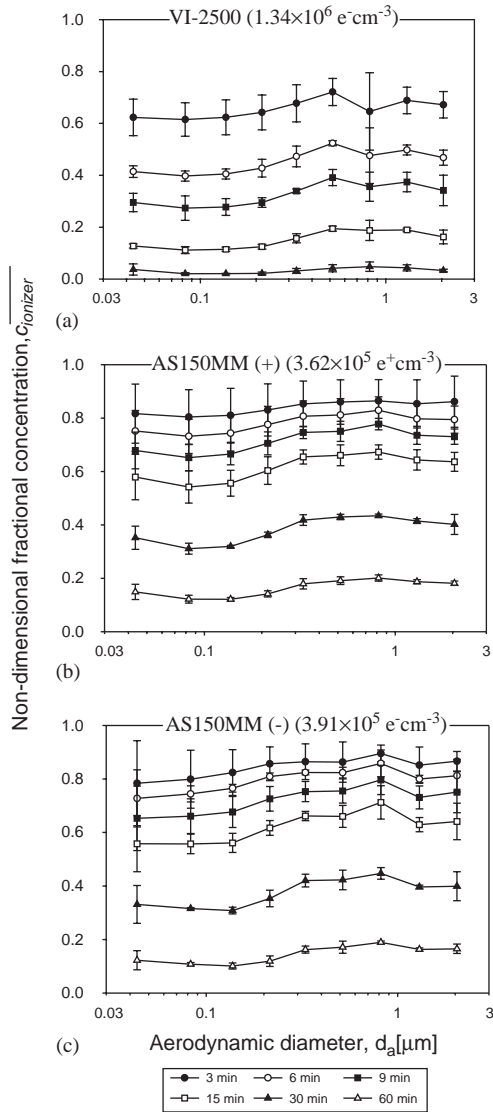


Fig. 3. The evolution of the non-dimensional particle fractional aerosol concentration during the operation of ion emitters: (a) VI-2500, (b) AS150MM (+), and (c) AS150MM (-). The error bars represent the standard deviations of 3 replicates.

24% for VI-2500, AS150MM (+), AS150MM (-) ion emitters, respectively. The theory underestimated the electric charge level for larger particles and overestimated it for smaller ones. The theoretical calculations utilized exclusively the diffusion charging model, as no external electric field was applied in our experimental setting. However, the ion densities produced by the emitters were so high that the ion flux itself could have generated a significant space electric field. The ion-induced space field might have resulted in additional charging of particles. For our experimental condition, we estimated that the field charging becomes

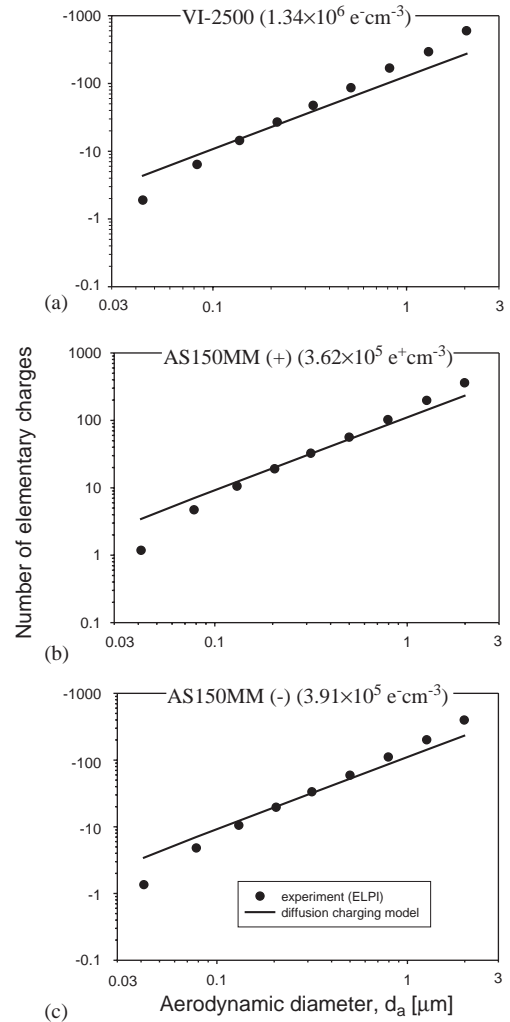


Fig. 4. The particle electric charge distributions, as measured by the ELPI and calculated based on the diffusion charging model (Hinds, 1999), respectively for each ion emitter: (a) VI-2500, (b) AS150MM (+), and (c) AS150MM (-). For experimental data, the standard deviation (of 3 replicates) did not exceed 6%; thus, the error bars are too small to be seen in the graphs.

significant relative to the diffusion charging when the particles are larger than  $\sim 1 \mu\text{m}$ . Thus, the measured average electric charges of particles exceeding  $\sim 1 \mu\text{m}$  are greater than their calculated values. The difference between the experimental and theoretical values is more pronounced at higher ion emission rates (this difference was greater for VI-2500 than for AS150MM). This also can be attributed to the ion-induced space field, which should increase with increasing ion emission rate. The overestimation of the measured data by the diffusion charging model observed for ultrafine particles can be explained by the limitation of the theoretical model.

Indeed, while the model includes the ion concentration, it is insensitive to the particle concentration, assuming that the latter is much lower than the former. However, the concentration of ultrafine particles ( $\sim 10^5 \text{ cm}^{-3}$ ) established in our tests was comparable to the ion density ( $\sim 10^5\text{--}10^6 \text{ e}^\pm \text{ cm}^{-3}$ ). This could affect the particle-ion collision efficiency because some particles were not surrounded by a sufficient number of ions. Therefore, these particles had lower electric charges than is predicted by the diffusion charging model.

The real-time measurement of air ions showed that the ion density rapidly increased when the emitter began operating in the chamber. After reaching the saturation level within 10s, it stayed at that level while the continuous ion emission supplied new ions into the indoor air environment. For VI-2500 and AS150MM, once the ion emitter was turned off, the ion density dropped by a factor of 10–20 during about 10s and essentially reached the initial (background) level in 3 min. This reflects a very high electric charge dissipation caused by the interaction of air ions with indoor surfaces in the chamber.

The particle removal efficiency, which can be achieved by a corona discharge unipolar ion emitter, depends on the particle electric mobility,  $Z$ , and the electric field strength,  $E$ , created by the unipolar air ions. The mobility was calculated for the three ionic air purifiers tested in this study. The ELPI-measured particle size and electric charges were incorporated to the following equation (Hinds, 1999):

$$Z = \frac{C_c q(d_p)}{3\pi\eta d_p}, \tag{5}$$

where  $C_c$  is the slip correction factor;  $q(d_p)$  is an average electric charge of a particle that has a diameter  $d_p$  ( $q = ne$ ); and  $\eta$  is the air viscosity. Table 2 lists the electric mobility values, which were determined based on the particle charge distribution measured at  $t = 3$  min. The mobility changes very slowly with the time of ionization following the logarithmic function of the diffusion

charging model. From Eq. (4), if the air is ionized by the most powerful VI-2500 emitter, the particle electric charges increase on average only by approximately 34% while the ionization time increases 100-fold (from  $t = 3$  min to  $t = 300$  min = 6 h). Being proportional to the particle charge [see Eq. (5)], the mobility would also change by 34% in 6 h. Since in our experiments  $t = 1$  h, we concluded that the particle charge distribution measured at  $t = 3$  min is representative of the particle electric mobility during the entire 1-hour test.

It is seen from Table 2 that the particle electric mobility was not dependent on the particle size. This can be attributed to the combination of the space field charging (effective for larger particles) and the diffusion charging (effective for smaller ones). The suppressed effect of the particle size on their electric mobility can help explain why the decay of the non-dimensional fractional concentration was not dependent on the particle size (see Fig. 3).

To relate the particle electric mobility and the ion-induced electric field to the particle removal from the air, the particle drift velocity was calculated using the equation for the terminal particle electrostatic velocity,  $V_E$ , (Hinds, 1999):

$$V_E = ZE = \frac{C_c q(d_p) E}{3\pi\eta d_p}. \tag{6}$$

According to Grabarczyk (2001), the ion emission density levels achieved in our experiments should create a field strength of  $\sim 10^3$  to  $\sim 10^4 \text{ V m}^{-1}$ . The particle drift velocity, calculated assuming that the field is spatially uniformed, allowed estimating its drift time from the center of the test chamber to the wall (the chamber's characteristic dimension). With the ion density provided by the VI-2500 emitter, the drift time is  $\sim 12$  min. For the AS150MM units, it is  $\sim 45$  min. Thus, ideally, the operation of the VI-2500 unit should make the entire volume of the chamber particle-free in about 12 min, and the operation of AS150MM should result in the particle-free environment in approximately 45 min. This theoretical estimate of the particle removal efficiency is in a reasonable agreement with the experimental values, although no 100% air cleaning was actually achieved in our experiments. The measurement data suggested the following: a 12-minute operation of VI-2500 removed about 80–90% of particles and a 45-minute operation of AS150MM removed almost 80% of particles (see Fig. 3).

Overall, we concluded that the ionic air purifiers, which are capable of producing unipolar ion density levels of  $10^5\text{--}10^6 \text{ e}^\pm \text{ cm}^{-3}$ , can be efficient in controlling fine and ultrafine aerosol pollutants in indoor air environments. The efficiency depends on the ion emission rate, as the latter affects the particle mobility. The air volume of the microenvironment (or, to be more precise, its surface-to-volume ratio) is also an important

Table 2  
The electrical mobility calculated from the particle charge distribution measurement data

Aerodynamic particle diameter ( $\mu\text{m}$ )	Electrical mobility ( $\text{m}^2 \text{ V}^{-1} \text{ s}^{-1}$ )		
	VI-2500	AS150MM (+)	AS150MM (–)
0.04	$-2.5 \times 10^{-7}$	$1.5 \times 10^{-7}$	$-1.8 \times 10^{-7}$
0.1	$-2.6 \times 10^{-7}$	$1.9 \times 10^{-7}$	$-1.9 \times 10^{-7}$
0.2	$-2.3 \times 10^{-7}$	$1.6 \times 10^{-7}$	$-1.7 \times 10^{-7}$
0.5	$-2.3 \times 10^{-7}$	$1.5 \times 10^{-7}$	$-1.6 \times 10^{-7}$
1	$-2.6 \times 10^{-7}$	$1.6 \times 10^{-7}$	$-1.7 \times 10^{-7}$
2	$-3.3 \times 10^{-7}$	$2.0 \times 10^{-7}$	$-2.2 \times 10^{-7}$



factor affecting the particle removal efficiency. This becomes apparent when the data obtained in this study in a 24.3 m<sup>3</sup> chamber are compared to those measured in our previous study (Grinshpun et al., 2004), where the same ionic air purifiers were evaluated in a 10-fold smaller chamber (the particle size ranges tested in these two studies have an overlap between 0.3 and 2 μm). The data suggest that with increasing air volume, more time is needed to reach a certain air cleaning level. Thus, unipolar ionic air purifiers are especially efficient in confined spaces.

It should be acknowledged that continuous injection of air ions of a single polarity (unlike bi-polar ions) into an enclosed environment leads to the charge accumulation on insulating surfaces, which may cause occasional electrostatic discharges or other “static”-related problems, especially at low humidity levels. Certain treatments of indoor surfaces may help address this issue (to be tested in future studies). Another phenomenon that limits the use of some unipolar ion emitters for the indoor air purification is a production of by-products. For example, negative ion generators may produce excessive concentration of ozone and nitrogen oxides. Several methods (e.g., a soft-corona discharge technique) have been developed to keep the concentration of these by-products in the air below conventionally accepted thresholds.

#### 4. Conclusions

Continuous emission of unipolar ions (either positive or negative), which is capable of creating an ion density of 10<sup>5</sup>–10<sup>6</sup> e<sup>±</sup> cm<sup>-3</sup>, can be efficient in controlling fine and ultrafine aerosol pollutants in indoor air environments, such as a typical office or residential room. The particles are charged primarily by the diffusion charging mechanism. At a high ion emission rate, the particle mobility becomes sufficient so that the particle migration results in their deposition on the walls and other indoor surfaces. Within the experimental conditions, the particle size effect on the mobility is suppressed and thus the particle removal efficiency is about the same for the fine and ultrafine particle size ranges. The particle removal depends on the ion emission rate and the time of emission. The indoor air volume is also a factor affecting the performance of an ion emitter.

Three ionic air purifiers, which produce unipolar ions by corona discharge at relatively high emission rates, were tested in this study through a real time aerosol monitoring and found efficient to remove fine and ultrafine aerosol particles from the air of a typical room. A 30-minute operation of the most powerful ion emitter (VI-2500) removed about 97% of 0.1 μm particles and about 95% of 1 μm particles from the air in addition to the natural decay effect. A 60-minute operation of two

other emitters [AS150MM (+) and AS150MM (-)] in the same environment removed about 83% and 84% of 0.1 μm particles and about 79% and 83% of 1 μm particles, respectively.

#### Disclaimer

Reference to any companies or specific commercial products does not necessarily constitute or imply their endorsement, recommendation, or favoring by the University of Cincinnati.

#### Acknowledgements

The participation of Dr. Lee in this study was partially supported by the Post-doctoral Fellowship Program of the Korea Science & Engineering Foundation (KOSEF). The KOSEF's support is very much appreciated. The authors also owe debts of gratitude to Ms. Alexandra Appatova for her essential help in editing the manuscript.

#### References

- Adachi, M., Kousaka, Y., Okuyama, K., 1985. Unipolar and bipolar diffusion charging of ultrafine aerosol particles. *Journal of Aerosol Science* 16, 109–123.
- Baron, P.A., Willeke, K., 2001. *Aerosol Measurement: Principles, Techniques, and Applications*. Wiley, New York.
- Buscher, P., Schmidt-Ott, A., Wiedensohler, A., 1994. Performance of a unipolar ‘square wave’ diffusion charger with variable nt-product. *Journal of Aerosol Science* 25, 651–663.
- Cheng, Y.S., Bechtold, W.E., Yu, C.C., Hung, I.F., 1995. Incense smoke: characterization and dynamics in indoor environments. *Aerosol Science and Technology* 23, 271–281.
- Choe, K.T., Trunov, M., Grinshpun, S.A., Willeke, K., Harney, J., Trakumas, S., Mainelis, G., Bornschein, R., Clark, S., Friedman, W., 2000. Particle settling after lead-based paint abatement work and clearance waiting period. *American Industrial Hygiene Association Journal* 61, 798–807.
- Grabarczyk, Z., 2001. Effectiveness of indoor air cleaning with corona ionizers. *Journal of Electrostatics* 51–52, 278–283.
- Grinshpun, S.A., Choe, K.T., Trunov, M., Willeke, K., Menrath, W., Friedman, W., 2002. Efficiency of final cleaning for lead-based paint abatement in indoor environments. *Applied Occupational and Environmental Hygiene* 17, 222–234.
- Grinshpun, S.A., Mainelis, G., Reponen, T., Willeke, K., Trunov, M.A., Adhikari, A., 2001. Effect of wearable ionizers on the concentration of respirable airborne particles and microorganisms. *Journal of Aerosol Science* 32, S335–S336.
- Grinshpun, S.A., Mainelis, G., Trunov, M., Adhikari, A., Reponen, T., Willeke, K., 2004. Evaluation of ionic air

- purifiers for reducing an aerosol exposure in confined indoor spaces. *Indoor Air*, submitted for publication.
- Hernandez-Sierra, A., Alguacil, F.J., Alonso, M., 2003. Unipolar charging of nanometer aerosol particles in a corona ionizer. *Journal of Aerosol Science* 34, 733–745.
- Hinds, W. C., 1999. *Aerosol Technology: Properties, Behavior, and Measurement of Airborne Particles*, Second Edition. A Wiley-Interscience publication, New York (Chapter 1, 3, 9, 15).
- Jamriska, M., Morawska, L., Ristovski, Z., 1998. Performance assessment of electrostatic filters with a focus on sub-micrometer particles. *Journal of Aerosol Science* 29, S1129–S1130.
- Klepeis, N.E., Nelson, W.C., Ott, W.R., Robinson, J.P., Tsang, A.M., Switzer, P., Behar, J.V., Hern, S.C., Engelmann, W.H., 2001. The National human activity pattern survey (NHAPS): A resource for assessing exposure to environmental pollutants. *Journal of Exposure Analysis and Environmental Epidemiology* 11, 231–252.
- Krueger, A.P., Reed, E.J., 1976. Biological impact of small air ions. *Science* 193, 1209–1213.
- Ludwig, J.F., Turner, W., 1991. In: Samet, J.M., Spengler, J.D. (Eds.), *Control strategies in indoor air pollution: a health Perspective*, pp. 351–377.
- Niu, J.L., Tung, T.C.W., Burnett, J., 2001. Quantification of dust removal and ozone emission of ionizer air-cleaners by chamber testing. *Journal of Electrostatics* 51–52, 20–24.
- Vincent, J.H., 1995. *Aerosol Science for Industrial Hygienists* Elsevier Science Inc. New York, USA.
- Wiedensohler, A., Buscher, P., Hansson, H.C., Martinsson, B.G., Stratmann, F., Ferron, G., Busch, B., 1994. A novel unipolar charger for ultrafine aerosol particles with minimal particle losses. *Journal of Aerosol Science* 25, 639–649.